Applied Surface Science Advances 5 (2021) 100111

Contents lists available at ScienceDirect

Applied Surface Science Advances

journal homepage: www.sciencedirect.com/journal/applied-surface-science-advances

Encapsulation of cells in gold nanoparticle functionalized hybrid Layer-by-Layer (LbL) hybrid shells – Remote effect of laser light

Louis Van der Meeren [a], Joost Verduijn [a], Jie Li [a], Ellen Verwee [a], Dmitri V. Krysko [b,c], Bogdan V. Parakhonskiy [a], Andre G. Skirtach [a,b,*]

[a] Nano-Biotechnology Laboratory, Department of Biotechnology, Ghent University, Ghent 9000, Belgium
[b] Cancer Research Institute Ghent, Ghent 9000, Belgium
[c] Cell Death Investigation and Therapy (CDIT) Laboratory, Department of Human Structure and Repair, Ghent University, Ghent 9000, Belgium

ARTICLE INFO

Keywords:
Layer-by-layer
LbL
Cells
Encapsulation
Viability
Nanoarchitectonics
Laser
Remote
Nanoparticles

ABSTRACT

Encapsulation of cells has been an active area of research. Among various methods for encapsulation, Layer-by-Layer (LbL) offers extensive flexibility in the design of surfaces and their interfacial nanoarchitectonics. A diverse range of functionalities have been recently demonstrated for cell encapsulation including protection and improved circulation. Here, we present a new strategy of cell encapsulation in a hybrid coating containing LbL assembly functionalized with gold nanoparticle aggregates. The effect of this hybrid coating on cell viability was assessed. Subsequently, upon laser illumination the encapsulated cells undergo immediate necrosis caused by the localized heat generated by the laser beam on gold nanoparticle aggregates. Similarly to affecting polyelectrolyte multilayer capsules, one envisions controlling surface properties of cells remotely by a laser beam. Further applications of the proposed approach are expected to be in biomedicine.

1. Introduction

Cell encapsulation is an active area of research, where various approaches exist, among which are fibrous coverage, hydrogel, the Layer-by-Layer (LbL) assembly. The latter represents a flexible way of covering cells, due to possibilities of choosing the type of polymers, the number of polymers in the polyelectrolyte shell, incorporation of various molecules and nanoparticles in the shell.

Originally, the LbL assembly has been applied on flat surfaces [1] for thin layer deposition [2], later coatings and thick, exponentially grown layers have been reported [3]. Applications interesting and attractive for biology have been developed including LbL coatings and polyelectrolyte multilayer capsules [4]. What makes the LbL assembly unique is the availability of various stimuli for controlling encapsulation, release, and manipulation due to the properties of different polymers [5]. Therefore, it is important to study fundamental principles of the LbL assembly [6–8], which enables design of surfaces with unprecedented precision in the so-called nanoarchitectonics assembly [9]. Eventually, the LbL assembly has been transferred to spherical particles serving as sacrificial templates. In the area of polyelectrolyte multilayer capsules, intracellular delivery functionalities [10], sensing and biosensing [11,12] corrosion protection [13,14] are some application areas.

LbL-coating was also already extensively combined with cell research, here two major approaches are known. In the first approach, nanoparticles are coated to assess the changes in interactions with cells, which can be explored in many biological applications. This strategy was used to either decrease the toxic effects from certain nanoparticles on cells (e.g. superparamagnetic particles [15], gold nanoparticles [16]) or rather increase the toxic effect [17]. This approach was also used to create a strong association between neuronal progenitor cells and magnetic nanoparticles allowing manipulate the location of the cells [18]. In alternative approach, LbL assembly is used for directly coating cells [19,20], later using them to serve as natural templates for polyelectrolyte multilayer assembly [21,22], where red blood cells were some of the first cells for assembly [15]. In addition, cells were coated for protection when using them in sensors and biosensors [23]. A good viability of cells coated with LbL assembly has been reported [24]. Since then, the range of applications of LbL coated cells has been extended [25,26]. Such interesting functionalities as improved circulation in blood stream was demonstrated [27], while in another application protection of cells has been achieved for long periods of time after their coating with the LbL assembly [28]. In another example, T cells were

* Corresponding author at: Nano-Biotechnology Laboratory, Department of Biotechnology, Ghent University, Ghent 9000, Belgium.
E-mail address: Andre.Skirtach@UGent.be (A.G. Skirtach).

https://doi.org/10.1016/j.apsadv.2021.100111
Received 3 January 2021; Received in revised form 15 May 2021; Accepted 31 May 2021
Available online 15 June 2021

coated with synthetic polyelectrolytes (namely polystyrene sulfonate and polyallylamine hydrochloride) also containing gold nanorods and resulting in a more inert T cell population for immunotherapy and biomedical applications [29]. Coating of micro-organisms has been conducted with the LbL assembly [30]. It can be noted that mimicking cells [31] can be also done with LbL assembly, which adds additional capability in comparison with polymeric capsules [32]. Although various methods of LbL assemblies exist [33,34] including spraying [35–37], traditionally used coating and washing procedure [38] is best applicable for coating cells.

Developing hybrid organic-inorganic materials opens extensive opportunities for designing versatile materials [39], and LbL assembly has been no exception [40–42]. Bringing in very different functionalities by polymers, which represent an organic component, and nanoparticles, which belong to inorganic materials, enable realization of different applications. For example, nanorods have been used as pH sensors [43]. In regard with nanoparticles, an attractive application is to target such polymeric assemblies as planar layers or spherical nanoparticles with a laser beam. Noble metalnanoparticles have been shown to convert light into heat, and this effect depends on the concentration of nanoparticles and intensity of the laser beam [44]. As it is described above, this principle has been applied to various polyelectrolyte multilayer assemblies [45–50]. But, to the best of our knowledge, the laser action on nanoparticle functionalized encapsulated cells has not been reported to date.

In this work, we have coated MCA205 fibrosarcoma cells with polyelectrolyte multilayer coatings (Poly-L-arginine (P-Arg) (positive layer) and 1:1 mixture of dextran sodium sulphate (DSS):Tetramethylrhodamine isothiocyanate–Dextran (TRITC-Dextran) (negative layer)) using the LbL assembly method. In the coatings, gold nanoparticles (AuNP) have been introduced. Characterization of nanoparticles has been performed by atomic force microscopy, while fluorescence microscopy images confirmed the coatings of polymers on the surface of cells, whose viability was investigated The assembly performed in this work has been carried out with the purpose to make cells responsive to remote action of near-IR laser light (785 nm wavelength, situated in the phototherapeutic window thus leaving normal tissue unharmed [51]), which was subsequently used to remotely affect the coated cancer cells.

2. Materials and methods

2.1. Synthesis of AuNP

The AuNPs were synthesised following a previously published protocol [52]. Briefly, an aqueous solution of 30 mM $HAuCl_4$ (Sigma Aldrich, product number: 520918) was added to a solution of $C_{32}H_{68}BrN$ (Sigma Aldrich, product number 294136) (25 mM) in 80 mL of toluene (Sigma Aldrich). In a couple of seconds, a phase transfer of the metal salt can be noticed to the toluene phase. A reduction of the mixture is forced by adding a 0.4 M solution of $NaBH_4$ (Sigma Aldrich)(25 mL). After separation of the two phases, the toluene phase (containing the nanoparticles) is washed with 0.1 M H_2SO_4, 0.1 M NaOH (Sigma Aldrich) and H_2O three times subsequently and finally dried over anhydrous Na_2SO_4 (Sigma Aldrich).

2.2. Size analysis of AuNP

Size analysis of the AuNPs was performed using atomic force microscopy (AFM) imaging. For all images, the JPK-bioAFM Nanowizard 4 (Bruker, Germany) was used. The images were made in AC-mode (non-contact imaging mode) at 0.8 Hz and a set point of 22 nm. The cantilever used during these imaging experiments had a nominal spring constant of 40 N/m (cantilever n° 4 on the chip: AIO, BudgetSensors). To visualize the gold nanoparticles, 25 μL of a solution of 3.63×10^{11} AuNPs/mL was dried onto freshly cleaved mica.

2.3. Coating of cells

During the coating experiments, mouse fibrosarcoma MCA205 cells were used. These cells are a murine fibrosarcoma cells often used for studying the immune response to tumour cells and development of targeted cancer immunotherapies [53]. These cells were cultured in a Roswell Park Memorial Institute (RPMI) 1640 (Lonza) medium with addition of 10% FBS (Lonza), 1% Pen/Strep (Lonza) and 1 mM sodium pyruvate (Sigma-Aldrich). For the coating experiment, 5×10^6 MCA205 cells were used during the experiment. The positive polyelectrolyte poly-L-arginine (P-Arg, Sigma Aldrich) is added as the first layer at the concentration of 0.1 mg/mL in Hank's Balanced Salt Solution (HBSS, Sigma-Aldrich). Cells are incubated for 15 min in this solution, after which the coated cells are centrifuged for 5 min at 1000 RPM and washed three times using HBSS. The second layer is a mixture of a negative polyelectrolyte and a fluorescently labelled polymer (TRITC--dextran:dextran sodium sulphate (DSS) in a 1:1 ratio, Sigma-Aldrich), which is also dissolved in HBSS. The same experimental steps, as those for the poly-L-arginine, are executed here as well. For every subsequent layer, one of the previous steps is repeated in alternating order. In the last series of experiments, AuNPs were trapped in between different polyelectrolyte polymer layers. AuNPs were added after the first dextran layer (negatively charged) at a concentration of 5×10^{11} particles/mL in HBSS. For this coating layer, the same experimental steps were used as those for the polyelectrolyte layers: incubation of 15 min with the AuNPs followed by a 5 min centrifugation at 1000 RPM (rounds per minute) and three subsequent washes with HBSS.

2.4. Visualization of coated cells and image processing

Fluorescent imaging of the coated cells was performed using a Nikon Ti eclipse microscope. The added label is Hoechst33342 (1 μg/mL, Thermofisher). All further image processing steps have been performed in the software program ImageJ using custom macro's.

2.5. Effect of coating on the cell viability

Viability tests were performed on cells using the PrestoBlue cell viability assay. To perform these tests cells were seeded in 96 wells plate to a volume of 180 μl. To measure the viability, 20 μL of reagent is added to the wells containing cells and incubated for 3 h. Fluorescence was measured using the Tecan infinite 200Pro (560 nm excitation wavelength and 635 nm emission wavelength). To be able to determine the number of viable cells that correspond to the fluorescent signal, a standard curve was also included in these experiments (1000, 2500, 5000, 10000, 20000 cells, please refer to Supporting Information Fig. S1).

2.6. Laser action on cells coated with polymeric LbL assembly and AuNP

To analyse the effect of the laser light on the cells LbL-coated cells containing AuNPs, the cells were exposed to a near-infrared laser with the wavelength of 785 nm. The incident power of the laser was 80 mW. Encapsulated cells with AuNP aggregates were exposed to this laser for a duration of 5 s. The objective used during these experiments was a 63x WI/NA 1.0 (Nikon).

3. Results and discussion

The general course of experiments is depicted in Fig. 1. Initially, polyelectrolytes had to be chosen and we opted for more biocompatible polymers [54]:DSS and P-Arg. Assessing that cells have predominantly negatively charged surfaces [55]; we have thus started the LbL assembly with the positively charged polyelectrolyte, P-Arg. And the LbL assembly has been conducted sequentially, alternating P-Arg with a mixture of DSS:TRITC-Dextran (1:1 ratio), where both polyelectrolytes had similar

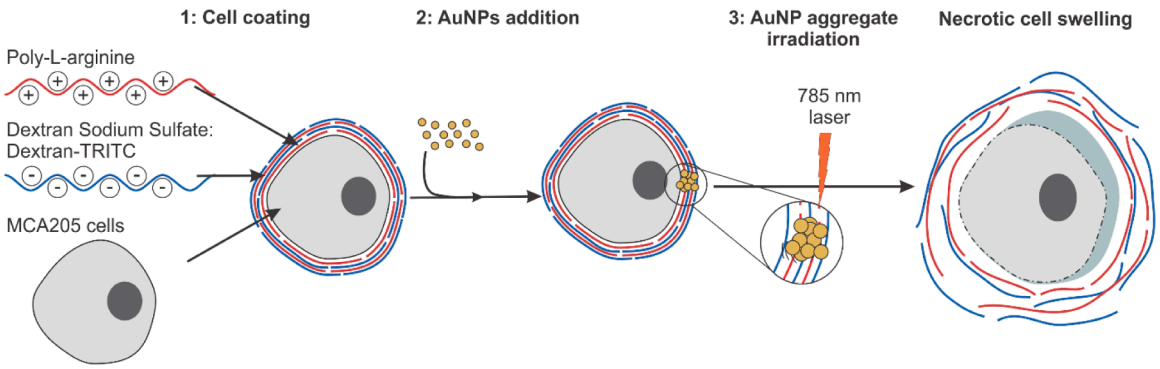

Fig. 1. Schematic representation of hybrid LbL-AuNP coatings around cells. By exposing LbL-coated cells with gold nanoparticle aggregates to a 785 nm laser, a strong localized heating can be induced resulting in necrotic cell swelling. To achieve an LbL-coating alternating postively and negatively charged polyelectrolytes are used. Here, the positively charged polyelectrolyte is poly-L-arginine (P-Arg) and negatively charged polyelectrolyte is composed of a 1:1 mixture of DSS and TRITC-Dextran.

molecular weights. Nanoparticle aggregates are incorporated in the coatings between the LbL assembled layers with the final goal to be able to destroy the coated cells by a laser beam (Fig. 1). Although both silver and gold nanoparticles have been used in the past [38], we have chosen gold nanoparticles for this study due to their stability.

3.1. Gold particle characterization

To allow cell illumination with laser, AuNPs need to be brought into close contact with cells. To achieve a permanent association between the cells and the gold nanoparticles aggregates, the cells can be coated in a LbL-manner [38], and gold particles can be trapped in between these coatings (due to their inherent positive charge) [52]. An important first step is to characterize gold nanoparticles. Initially, we have immobilized aggregated nanoparticles, which allows their easier visualization, and which is necessary for generating near-IR absorbance [56]. AuNP size analysis was performed with AFM imaging in constant amplitude mode (AC mode, Fig. 2A). It was possible to measure that the average size of aggregated AuNPs is ~ 65 nm (+/- 19 nm, $n = 100$) (Fig. 2B). Interestingly, when analysing the AFM phase shift images, the AuNPs can even be discerned more clearly, because AFM phase shift images provide contrast based on different chemical properties of materials.

Using previously published data combined with the measured diameter from the AFM experiments, it was possible to determine the concentration of the AuNPs from the absorbance at 450 nm (Supporting Information Fig. 2) [57]). Using these data we could conclude that the original concentration of the particles was: 1.60×10^{13} particles/ml [57]. These calculations are important for knowing how many gold nanoparticles are adsorbed in the cell coatings.

3.2. Cell polyelectrolyte LbL-coating

To effectively attach AuNPs on the cellular surface, cells were coated first with polyelectrolyte polymers. Adding layers of polyelectrolyte polymers ensures a strong association of the AuNPs with the cells. In the first approach, cells were coated using poly-L-arginine (MW = 15.000–70.000, ("+": a positively charged polyelectrolyte)) and a 1:1 mixture of DSS and TRITC-dextran (MW > 70.000, ("-": a negatively charged polyelectrolyte)), based on a previously presented and generalized protocols [58]. The positively charged polymer is used as the first layer since mammalian cells have an inherent negative charge on their membrane [55]. Usage of TRITC-dextran allows to confirm if coating of the cells is successful using fluorescence microscopy. After adsorbing 4 layers of polyelectrolytes, the cells were stained with Hoechst33342 (nucleus stain) and imaged using fluorescence microscopy (Fig. 3). From these images, the following observations can be made, cells are still present after the coating protocol, which is indicated by the Hoechst33342 stain (Fig. 3C). Furthermore, the red circle around the cells indicate that cells are successfully coated with the TRITC-Dextran polymer (Fig. 3B).

3.3. Cell viability experiments

The effect of the single cell coating on the viability of the cells was tested using the PrestoBlue assay. Two different conditions were investigated, namely: cells coated solely with polymers (denoted as Coated) and cells coated with polymers with adsorbed AuNPs aggregates in the 3rd layer (denoted as Gold-Coated). These coated cells were seeded into 5 wells of a 96 well plate (1000 cells/well). Of the 1000 seeded cells a viability of 86 % and 83 % was measured 4 h after coating for the polyelectrolyte-AuNP-coated and the polyelectrolyte-coated cells,

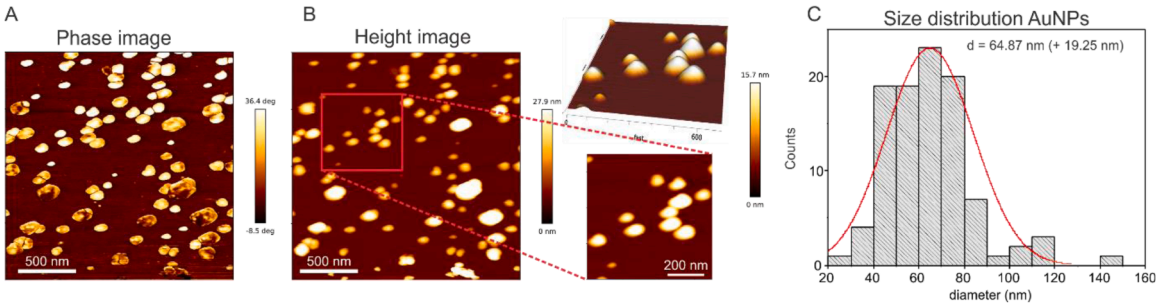

Fig. 2. AuNP characterization deposited on mica substrate. (A) AFM phase image of AuNPs and small AuNP aggregates, materials with a similar chemical compisition show a similar phase shift. (B) Left: height image of AuNPs and small AuNP aggregates. Right: zoom-in on individual AuNPs. (C) From the AFM images the size distribution (the diameter of the nanoparticle aggregates) is obtained, revealing the average value of ~ 65 nm.

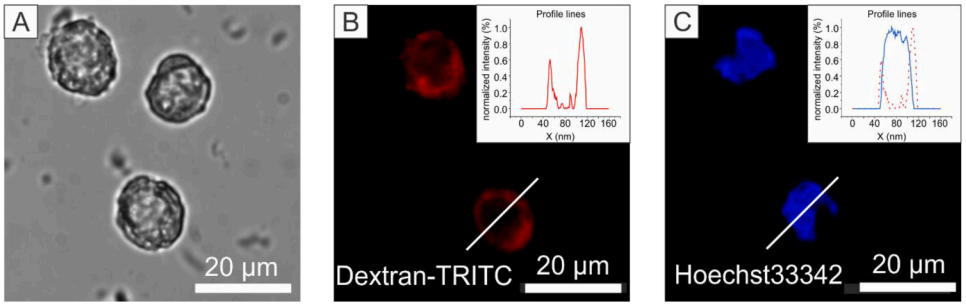

Fig. 3. Microscopy images of LbL-coated cells (the scale bar = 20 µm). (A) A transmission microscopy image of 3 coated MCA205 cells. (B) Fluorescence microscopy images: the red fluorescence channel showes the TRITC-labelled dextran proving the successful cell coating. Inset graphs show profile lines (white line) through the coated cell, the red full line represents the Dextran-TRITC signal. (C) The blue fluorescence channel showing the Hoechst33342 label indicating the presence of cellular nuclei inside the coatings. Inset graph shows a profile line through the coated cell (white line), the red dashed line represents the TRITC-Dextran signal, the blue full line represents the Hoechst33342 signal (For interpretation of the references to color in this figure legend, the reader is referred to the web version of this article.).

respectively. The viability was measured again 24 h after performing the coating. The number of viable cells increased significantly to 2659 (± 578) for the gold-nanoparticle coated cells and 2020 (± 441) for the coated cells. This translates to 3.1 and 2.3 times increase, respectively (Fig. 4A, B). In this 24 h period, the control cells exhibited 5.2 times increase (Fig. 4C). This discrepancy between coated and un-coated cells can be potentially explained due to the limitation of the division capacity of cells caused by the coating. However, the most important observation following from these experiments is that most cells are still viable.

The fact that surface coatings affects toxicity of gold nanoparticles has been reported previously [16,17,59]. However, the most important observation following from these experiments is that most cells is still viable. Similar data on a higher cell viability of cells and irradiated cells were found by others [60].

3.4. Effect of near-IR laser light on LbL-coated cells containing AuNP

In this work specifically, we are interested in the absorbance in the phototherapeutic window, where the human tissue is most transparent, and light has the most penetration (650–850 nm) [61]. During these experiments a laser with the wavelength of 785 nm is used (which situates comfortably in this window). Absorbance of the individual particles at this wavelength was measured using UV-Vis spectrometry. The individual AuNPs have a low absorbance at these higher wavelengths ($Abs_{785} = 0.36$ at the concentration of 7.98×10^{12} particles/ml) (Supporting Information Fig. S2). However, research has revealed that upon aggregation of these particles, the absorption at higher wavelengths increases significantly [62]. Interestingly, when coating the cells with gold nanoparticles, the buffer in which cells are present leads to gold nanoparticle aggregation due to screening of charges because of the presence of salt [54]. Previously, it has been shown that upon illumination of gold nanoparticles by a laser, light energy is converted to heat leading to a localized temperature rise [44]. Furthermore, it was also shown that by shortly illuminating AuNPs with a strong laser, a very local explosion can be induced either by a continuous wave (CW) [63] or pulsed laser [64,65] irradiation. In this research, we extend this idea by establishing a permanent strong link between the AuNPs and cells. This allows further manipulating, functionalizing and directing cells without concerns about AuNPs. The necessity for adsorbing the preceding polymer layers (before gold nanoparticles) is proven by the following experiment: when only AuNPs were added to the cells and subsequently centrifuged, no definitive associations between cells and AuNP aggregates were observed (data not shown).

In Fig. 5A, control cells are shown without AuNP aggregates. Incidence of a near-IR laser (785 nm, 80 mW power) for a duration of 30 s does not show any effect on the cellular morphology, which proves the important statement that these wavelengths do not affect normal tissue. This is consistent with previous studies, where no adverse effects were found by exposing cells to a near-IR laser [66]. In Fig. 5B and C, it is shown that a short irradiation of a AuNP aggregate (5 s, 80 mW power) leads to a significant morphology change in the targeted cell. The AuNP aggregates can be distinguished as a dark opaque dot in transmission microscopy (due to their broad absorbance spectrum). In Fig. 5B a coated cell can be observed where a AuNP aggregates are added *in situ*, here the irradiation of the AuNP aggregate results in an instantaneous

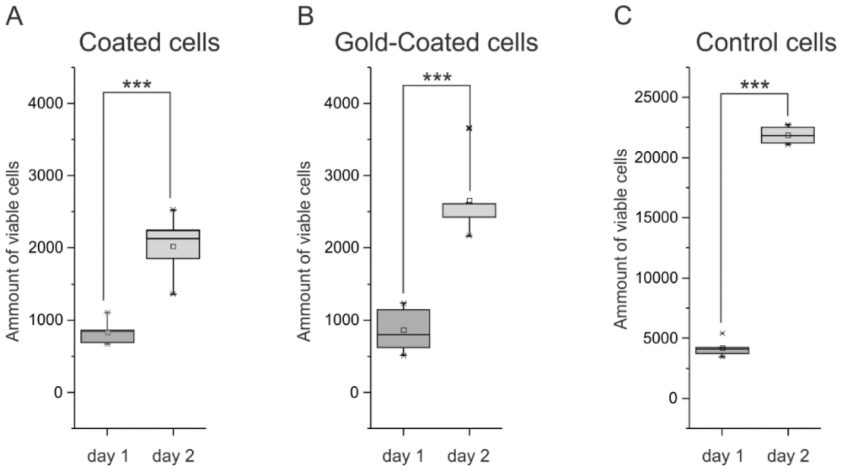

Fig. 4. Boxplot graphs showing results of the cell viability tests: (A) cells coated with 4 layers of polyelectrolytes. (B) cells coated with 3 layers of polymer and adsorbed AuNPs. (C) control cells without any coating. Significance was calculated using a T-test with unequal variance, *** = $p < 0.001$. A significant increase for the ammount of viable cells can be noticed for all conditions.

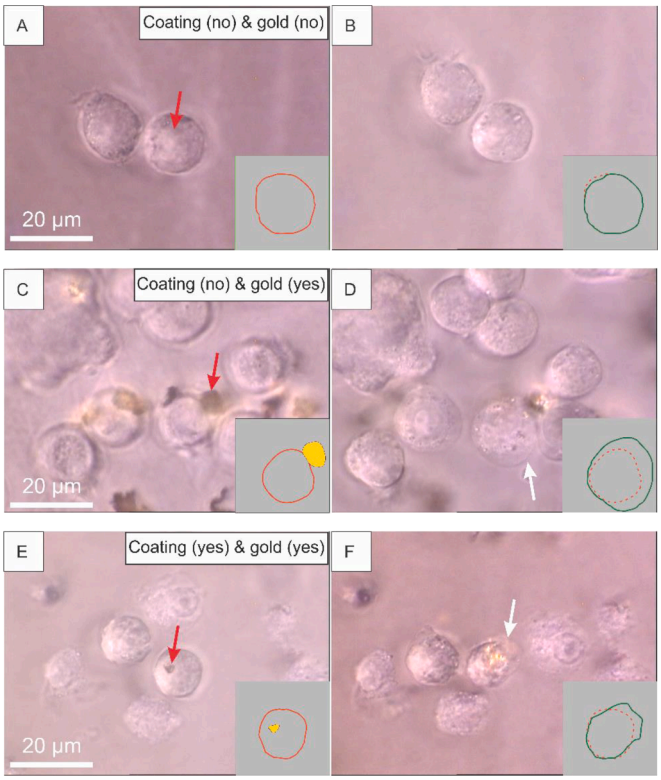

Fig. 5. Remote laser action on cells functionalized with hybrid LbL-AuNP aggreagtescoatings: (A) An uncoated control cell, inset (orange line on grey background) shows schematically the contour of the targeted cell. Red arrow indicates location of laser incidence. (B) The same targeted cell after laser irradiation; inset (green line on grey background) shows cellular contour after laser irradiation. No significant morphological changes can be observed. (C) Uncoated cell with in situ addition of AuNP aggregates before irradiation, inset (orange line) shows the contour of the cell and the targetted AuNP aggregate. The red arrow indicates location of laser incidence. (D) Targeted cell after laser irradiation inset (green line) shows cellular contour after remote action of laser on the AuNP aggregate. The white arrow indicates cell swelling and plasma membrane leakage typically associated with necrotic morphology. (E) LbL coated cell containing AuNP aggregates before laser irradiation, inset shows the contour of the cell (orange line) and the targetted AuNP aggregate. The red arrow indicates the location of laser irradiation. (F) The same targeted cell after laser irradiation inset (green line) shows cellular contour after AuNP aggregate explosion. White arrow indicates cell swelling and plasma membrane leakage typically associated with necrotic morphology (For interpretation of the references to color in this figure legend, the reader is referred to the web version of this article.).

cell swelling strongly resembling a necrotic state (i.e. cellular swelling and and absence of apoptotic bodies) [67]. The same laser incidence (5 s, 80 mW power) on a cell where AuNP is included in an LbL-coating leads to a similar response Fig. 5C. It can be noted that the morphological change in the uncoated cell (Fig. 5B) is stronger compared to the coated cell (Fig. 5C). A possible explanation for these observations can be twofold: firstly, the aggregate, which is activated by the laser, is significantly larger in the second example. Secondly it is likely that due to the LbL-coating of the cells, cell swelling is more constrained in the first example.

3.5. The influence of the aggregation state of nanoparticles and laser on nanoparticle coated cells

The state of nanoparticles affects the interaction of the laser with polymeric capsules or cells coated with light absorbing nanoparticles. A high density of coverage of nanoparticles results in an explosive effect as it was previously shown for microcapsules covered with silver nanoparticles [38], and as it is demonstrated here for cells covered with a high concentration of gold nanoparticles. The local character of laser-nanoparticle interaction has been recently discussed [68], where the global temperature rise, used among others for encapsulation and polyelectrolyte multilayer capsule shrinkage, has been contrasted to local effects of increased temperature, used for localized heating and release of encapsulated materials. In this work, we at remote cell death induction, but we note that decreasing the concentration of nanoparticles and laser powers would lead to a more local effect [69]. Most essential, controlling the nano-assembly of nanoparticles should allow one to choose the desired action. Remotely affecting cells demonstrated in this work will extend the already reported range of applications of cell encapsulation [70].

Furthermore, the results of these experiments provide interesting and new approaches for future research towards a better understanding and development of immunotherapy applications [71], which are still poorly understood [72]. By being able to induce cell death very locally and carefully (as we show here with the AuNP coated cells), we open possibilities to investigate interactions very specifically with the dead cells with the cells of the immune system. Furthermore, the demonstrated approach can be used for killing cells and bacteria [73] and also combined with capsules embedded in coatings and layers for their remote opening [74].

4. Conclusions

In this work, we have coated cancer fibrosarcoma MCA205 cells with polyelectrolyte multilayer shell using the Layer-by-Layer (LbL) assembly method. The coating of cells has been verified by fluorescence microscopy visualising a fluorescently labelled polymer, namely TRITC-dextran, used in the LbL assembly on cells. During the assembly of polyelectrolytes, gold nanoparticles in the form of aggregates have been incorporated into the layers. Incorporated AuNPs aggregates are capable of absorbing laser light and converting it to heat – this effect is used for destroying cancer cells coated with hybrid polyelectrolyte gold nanoparticles shell. Cell viability is studied revealing that in the LbL-AuNP-coated cells are viable. Upon exposure to a laser operating in a biologically “friendly” near-infrared spectral window, nanoparticle aggregates absorb light and convert it to heat, thus affecting the cells. In future, we anticipate controlling the surface properties, and as a result, the remote effect of laser on cells. The presented here results offer further opportunities for extending the range of application of the LbL assembly, which has been extensively pursued by Helmuth Möhwald [4].

Declaration of Competing Interest

The authors declare that they have no competing interests.

Acknowledgments

We acknowledge the Fund for Scientific Research (FWO) Flanders (I002620N, GO16221N, G043219N) and the Ghent University BOF (Special Research Fund; IOP 01/O3618, BAS094-18, BOF14/IOP/003). B.V.P. is FWO post-doctoral fellow. J.L. acknowledges support of the China Scholarship Council (CSC). E.V. and A.G.S. also thank the support of the SBO project EffSep.

Supplementary materials

Supplementary material associated with this article can be found, in the online version, at doi:10.1016/j.apsadv.2021.100111.

References

[1] G. Decher, Fuzzy nanoassemblies: toward layered polymeric multicomposites, Science 277 (1997) 1232–1237, https://doi.org/10.1126/science.277.5330.1232.

[2] Y. Lvov, K. Ariga, T. Kunitake, I. Ichinose, Assembly of multicomponept protein films by means of electrostatic layer-by-layer adsorption, J. Am. Chem. Soc. 117 (1995) 6117–6123, https://doi.org/10.1021/ja00127a026.

[3] P. Lavalle, C. Gergely, F.J.G. Cuisinier, G. Decher, P. Schaaf, J.C. Voegel, C. Picart, Comparison of the structure of polyelectrolyte multilayer films exhibiting a linear and an exponential growth regime: an in situ atomic force microscopy study, Macromolecules 35 (2002) 4458–4465, https://doi.org/10.1021/ma0119833.

[4] S. Zhao, F. Caruso, L. Dahne, G. Decher, B.G. De Geest, J. Fan, N. Feliu, Y. Gogotsi, P.T. Hammond, M.C. Hersam, A. Khademhosseini, N. Kotov, S. Leporatti, Y. Li, F. Lisdat, L.M. Liz-Marzan, S. Moya, P. Mulvaney, A.L. Rogach, S. Roy, D. G. Shchukin, A.G. Skirtach, M.M. Stevens, G.B. Sukhorukov, P.S. Weiss, Z. Yue, D. Zhu, W.J. Parak, The future of layer-by-layer assembly: a tribute to ACS Nano associate editor Helmuth Mohwald, ACS Nano 13 (2019) 6151–6169, https://doi.org/10.1021/acsnano.9b03326.

[5] M. Delcea, H. Möhwald, A.G. Skirtach, Stimuli-responsive LbL capsules and nanoshells for drug delivery, Adv. Drug Deliv. Rev. 63 (2011) 730–747, https://doi.org/10.1016/j.addr.2011.03.010.

[6] S.T. Dubas, J.B. Schlenoff, Swelling and smoothing of polyelectrolyte multilayers by salt, Langmuir 17 (2001) 7725–7727, https://doi.org/10.1021/la0112099.

[7] E. Kharlampieva, S.A. Sukhishvili, Ionization and pH stability of multilayers formed by self-assembly of weak polyelectrolytes, Langmuir 19 (2003) 1235–1243, https://doi.org/10.1021/la026546b.

[8] S. Dodoo, R. Steitz, A. Laschewsky, R. Von Klitzing, Effect of ionic strength and type of ions on the structure of water swollen polyelectrolyte multilayers, Phys. Chem. Chem. Phys. 13 (2011) 10318–10325, https://doi.org/10.1039/c0cp01357a.

[9] K. Ariga, S. Watanabe, T. Mori, J. Takeya, Soft 2D nanoarchitectonics, NPG Asia Mater. 10 (2018) 90–106, https://doi.org/10.1038/s41427-018-0022-9.

[10] M.V. Zyuzin, A.S. Timin, G.B. Sukhorukov, Multilayer capsules inside biological systems: state-of-the-art and open challenges, Langmuir 35 (2019) 4747–4762, https://doi.org/10.1021/acs.langmuir.8b04280.

[11] O. Kreft, A.M. Javier, G.B. Sukhorukov, W.J. Parak, Polymer microcapsules as mobile local pH-sensors, J. Mater. Chem. 17 (2007) 4471–4476, https://doi.org/10.1039/b705419j.

[12] L. Van der Meeren, J. Li, B.V. Parakhonskiy, D.V. Krysko, A.G. Skirtach, Classification of analytics, sensorics, and bioanalytics with polyelectrolyte multilayer capsules, Anal. Bioanal. Chem. (2020), https://doi.org/10.1007/s00216-020-02428-8.

[13] D.V. Andreeva, E.V. Skorb, D.G. Shchukin, Layer-by-layer polyelectrolyte/inhibitor nanostructures for metal corrosion protection, ACS Appl. Mater. Interfaces 2 (2010) 1954–1962, https://doi.org/10.1021/am1002712.

[14] D.V. Andreeva, D.V. Sviridov, A. Masic, H. Möhwald, E.V. Skorb, Nanoengineered metal surface capsules: construction of a metal-protection system, Small 8 (2012) 820–825, https://doi.org/10.1002/smll.201102365.

[15] Z. Ferjaoui, S. Nahle, C.S. Chang, J. Ghanbaja, O. Joubert, R. Schneider, L. Ferrari, E. Gaffet, H. Alem, Layer-by-Layer self-assembly of polyelectrolytes on superparamagnetic nanoparticle surfaces, ACS Omega 5 (2020) 4770–4777, https://doi.org/10.1021/acsomega.9b02963.

[16] S.T. Kim, K. Saha, C. Kim, V.M. Rotello, The role of surface functionality in determining nanoparticle cytotoxicity, Acc. Chem. Res. 46 (2013) 681–691, https://doi.org/10.1021/ar3000647.

[17] J. Deng, M. Yao, C. Gao, Cytotoxicity of gold nanoparticles with different structures and surface-anchored chiral polymers, Acta Biomater. 53 (2017) 610–618, https://doi.org/10.1016/j.actbio.2017.01.082.

[18] I. Guryanov, E. Naumenko, S. Konnova, M. Lagarkova, S. Kiselev, R. Fakhrullin, Spatial manipulation of magnetically-responsive nanoparticle engineered human neuronal progenitor cells, Nanomed. Nanotechnol. Biol. Med. 20 (2019), 102038, https://doi.org/10.1016/j.nano.2019.102038.

[19] H. Ai, M. Fang, S.A. Jones, Y.M. Lvov, Electrostatic Layer-by-Layer nanoassembly on biological microtemplates: Platelets, Biomacromolecules 3 (2002) 560–564, https://doi.org/10.1021/bm015659r.

[20] E.A. Naumenko, M.R. Dzamukova, R.F. Fakhrullin, Magnetically functionalized cells: fabrication, characterization, and biomedical applications. Implantable Bioelectronics, Wiley Blackwell, 2014, pp. 7–26, https://doi.org/10.1002/9783527673148.ch2.

[21] S. Moya, L. Dähne, A. Voigt, S. Leporatti, E. Donath, H. Möhwald, Polyelectrolyte multilayer capsules templated on biological cells: Core oxidation influences layer chemistry, Colloids Surf. A Physicochem. Eng. Asp. 183–185 (2001) 27–40, https://doi.org/10.1016/S0927-7757(01)00537-4.

[22] O. Kreft, R. Georgieva, H. Bäumler, M. Steup, B. Müller-Röber, G.B. Sukhorukov, H. Möhwald, Red blood cell templated polyelectrolyte capsules: a novel vehicle for the stable encapsulation of DNA and proteins, Macromol. Rapid Commun. 27 (2006) 435–440, https://doi.org/10.1002/marc.200500777.

[23] M. Germain, P. Balaguer, J.C. Nicolas, F. Lopez, J.P. Esteve, G.B. Sukhorukov, M. Winterhalter, H. Richard-Foy, D. Fournier, Protection of mammalian cell used in biosensors by coating with a polyelectrolyte shell, Biosens. Bioelectron. 21 (2006) 1566–1573, https://doi.org/10.1016/j.bios.2005.07.011.

[24] S.H. Yang, E.H. Ko, I.S. Choi, Cytocompatible encapsulation of individual chlorella cells within titanium dioxide shells by a designed catalytic peptide, Langmuir 28 (2012) 2151–2155, https://doi.org/10.1021/la203667z.

[25] T. Liu, Y. Wang, W. Zhong, B. Li, K. Mequanint, G. Luo, M. Xing, Biomedical applications of layer-by-layer self-assembly for cell encapsulation: current status and future perspectives, Adv. Healthc. Mater. 8 (2019), 1800939, https://doi.org/10.1002/adhm.201800939.

[26] Y. Choi, B. Phan, M. Tanaka, J. Hong, J. Choi, Methods and applications of biomolecular surface coatings on individual cells, ACS Appl. Bio Mater. 3 (2020) 6556–6570, https://doi.org/10.1021/acsabm.0c00867.

[27] J. Wang, Z. Sun, W. Gou, D.B. Adams, W. Cui, K.A. Morgan, C. Strange, H. Wang, α-1 antitrypsin enhances islet engraftment by suppression of instant blood-mediated inflammatory reaction, Diabetes 66 (2017) 970–980, https://doi.org/10.2337/db16-1036.

[28] J. Barra, H.M. Tse, Tannic acid–encapsulated islets suppress autoimmunity and restore euglycemia following transplantation, Diabetes 67 (2018), https://doi.org/10.2337/db18-29-or, 29-OR.

[29] P. Wattanakull, M.C. Killingsworth, D. Pissuwan, Biological responses of t cells encapsulated with polyelectrolyte-coated gold nanorods and their cellular activities in a co-culture system, Appl. Nanosci. 7 (2017) 667–679, https://doi.org/10.1007/s13204-017-0605-8.

[30] R.F. Fakhrullin, Y.M. Lvov, face-lifting" and "make-up" for microorganisms: layer-by-layer polyelectrolyte nanocoating, ACS Nano 6 (2012) 4557–4564, https://doi.org/10.1021/nn301776y.

[31] S. She, Q. Li, B. Shan, W. Tong, C. Gao, Fabrication of red-blood-cell-like polyelectrolyte microcapsules and their deformation and recovery behavior through a microcapillary, Adv. Mater. 25 (2013) 5814–5818, https://doi.org/10.1002/adma.201302875.

[32] T.A. Kolesnikova, A.G. Skirtach, H. Möhwald, Red blood cells and polyelectrolyte multilayer capsules: natural carriers versus polymer-based drug delivery vehicles, Expert Opin. Drug Deliv. 10 (2013) 47–58, https://doi.org/10.1517/17425247.2013.730516.

[33] J.J. Richardson, M. Bjornmalm, F. Caruso, Technology-driven layer-by-layer assembly of nanofilms, Science 348 (2015), https://doi.org/10.1126/science.aaa2491 aaa2491–aaa2491.

[34] J.J. Richardson, H. Ejima, S.L. Lörcher, K. Liang, P. Senn, J. Cui, F. Caruso, Preparation of nano- and microcapsules by electrophoretic polymer assembly, Angew. Chem. Int. Ed. 52 (2013) 6455–6458, https://doi.org/10.1002/anie.201302092.

[35] J.B. Schlenoff, S.T. Dubas, T. Farhat, Sprayed polyelectrolyte multilayers, Langmuir 16 (2000) 9968–9969, https://doi.org/10.1021/la001312i.

[36] P. Schaaf, J.C. Voegel, L. Jierry, F. Boulmedais, Spray-assisted polyelectrolyte multilayer buildup: from step-by-step to single-step polyelectrolyte film constructions, Adv. Mater 24 (2012) 1001–1016, https://doi.org/10.1002/adma.201104227.

[37] M. Dierendonck, S. De Koker, R. De Rycke, B.G. De Geest, Just spray it-LbL assembly enters a new age, Soft Matter 10 (2014) 804–807, https://doi.org/10.1039/c3sm52202d.

[38] A.G. Skirtach, A.M. Yashchenok, H. Möhwald, H. Möhwald, Encapsulation, release and applications of LbL polyelectrolyte multilayer capsules, Chem. Commun. (2011) 47, https://doi.org/10.1039/c1cc13453a.

[39] M.S. Saveleva, K. Eftekhari, A. Abalymov, T.E.L. Douglas, D. Volodkin, B. V. Parakhonskiy, A.G. Skirtach, Hierarchy of hybrid materials-the place of inorganics-in-organics in it, their composition and applications, Front. Chem. 7 (2019) 179, https://doi.org/10.3389/fchem.2019.00179.

[40] S. Srivastava, N.A. Kotov, Composite Layer-by-Layer (LBL) assembly with inorganic nanoparticles and nanowires, Acc. Chem. Res. 41 (2008) 1831–1841, https://doi.org/10.1021/ar8001377.

[41] P. Podsiadlo, M. Michel, J. Lee, E. Verploegen, N.W.S. Kam, V. Ball, J. Lee, Y. Qi, A. J. Hart, P.T. Hammond, N.A. Kotov, Exponential growth of LBL films with incorporated inorganic sheets, Nano Lett. 8 (2008) 1762–1770, https://doi.org/10.1021/nl8011648.

[42] E.V. Lengert, S.I. Koltsov, J. Li, A.V. Ermakov, B.V. Parakhonskiy, E.V. Skorb, A. G. Skirtach, Nanoparticles in polyelectrolyte multilayer layer-by-layer (LbL) films and capsules—key enabling components of hybrid coatings, Coatings 10 (2020) 1131, https://doi.org/10.3390/coatings10111131.

[43] V. Kozlovskaya, E. Kharlampieva, B.P. Khanal, P. Manna, E.R. Zubarev, V. V. Tsukruk, Ultrathin layer-by-layer hydrogels with incorporated gold nanorods as pH-sensitive optical materials, Chem. Mater. 20 (2008) 7474–7485, https://doi.org/10.1021/cm8023633.

[44] A.G. Skirtach, C. Dejugnat, D. Braun, A.S. Susha, A.L. Rogach, W.J. Parak, H. Möhwald, G.B. Sukhorukovt, The role of metal nanoparticles in remote release of encapsulated materials, Nano Lett. 5 (2005) 1371–1377, https://doi.org/10.1021/nl050693n.

[45] A.L. Becker, A.P.R. Johnston, F. Caruso, Layer-by-Layer-assembled capsules and films for therapeutic delivery, Small 6 (2010), https://doi.org/10.1002/smll.201000379 n/a-n/a.

[46] S. Anandhakumar, A.M. Raichur, Polyelectrolyte/silver nanocomposite multilayer films as multifunctional thin film platforms for remote activated protein and drug delivery, Acta Biomater. 9 (2013) 8864–8874, https://doi.org/10.1016/j.actbio.2013.06.012.

[47] J. Borges, L.C. Rodrigues, R.L. Reis, J.F. Mano, Layer-by-layer assembly of light-responsive polymeric multilayer systems, Adv. Funct. Mater. 24 (2014) 5624–5648, https://doi.org/10.1002/adfm.201401050.

[48] M.J. Feeney, S.W. Thomas, Combining top-down and bottom-up with photodegradable layer-by-layer films, Langmuir 35 (2019) 13791–13804, https://doi.org/10.1021/acs.langmuir.9b02005.

[49] A.S. Timin, D.J. Gould, G.B. Sukhorukov, Multi-layer microcapsules: fresh insights and new applications, Expert Opin. Drug Deliv. 14 (2017) 583–587, https://doi.org/10.1080/17425247.2017.1285279.

[50] K. Chojnacka-Górka, K. Wolski, S. Zapotoczny, Durable polyelectrolyte microcapsules with near-infrared-triggered loading and nondestructive release of cargo, ACS Appl. Mater. Interfaces 13 (2021) 1562–1572, https://doi.org/10.1021/acsami.0c19353.
[51] J.M. Dąbrowski, B. Pucelik, A. Regiel-Futyra, M. Brindell, O. Mazuryk, A. Kyzioł, G. Stochel, W. Macyk, L.G. Arnaut. https://doi.org/10.1016/j.ccr.2016.06.007.
[52] D.I. Gittins, F. Caruso, Spontaneous phase transfer of nanoparticulate metals from organic to aqueous media, Angew. Chem. Int. Ed. 40 (2001) 3001–3004, https://doi.org/10.1002/1521-3773(20010817)40:16<3001::AID-ANIE3001>3.0.CO;2-5.
[53] I. Efimova, E. Catanzaro, L. Van der Meeren, V.D. Turubanova, H. Hammad, T. A. Mishchenko, M.V Vedunova, C. Fimognari, C. Bachert, F. Coppieters, S. Lefever, A.G. Skirtach, O. Krysko, D.V Krysko, Vaccination with early ferroptotic cancer cells induces efficient antitumor immunity, J. Immunother. Cancer. 8 (2020), e001369, https://doi.org/10.1136/jitc-2020-001369.
[54] P. De Vos, H.A. Lazarjani, D. Poncelet, M.M. Faas, Polymers in cell encapsulation from an enveloped cell perspective, Adv. Drug Deliv. Rev. 67–68 (2014) 15–34, https://doi.org/10.1016/j.addr.2013.11.005.
[55] Pekker M., Shneider M.N., Interaction between electrolyte ions and the surface of a cell lipid membrane, (2015). 10.4172/2161-0398.1000177.
[56] M.F. Bédard, D. Braun, G.B. Sukhorukov, A.G. Skirtach, Toward self-assembly of nanoparticles on polymeric microshells: near-IR release and permeability, ACS Nano 2 (2008) 1807–1816, https://doi.org/10.1021/nn8002168.
[57] W. Haiss, N.T.K. Thanh, J. Aveyard, D.G. Fernig, Determination of size and concentration of gold nanoparticles from UV-Vis spectra, Anal. Chem. 79 (2007) 4215–4221, https://doi.org/10.1021/ac0702084.
[58] N.G. Veerabadran, P.L. Goli, S.S. Stewart-Clark, Y.M. Lvov, D.K. Mills, Nanoencapsulation of stem cells within polyelectrolyte multilayer shells, Macromol. Biosci. 7 (2007) 877–882, https://doi.org/10.1002/mabi.200700061.
[59] A. Albanese, P.S. Tang, W.C.W. Chan, The effect of nanoparticle size, shape, and surface chemistry on biological systems, Annu. Rev. Biomed. Eng. 14 (2012) 1–16, https://doi.org/10.1146/annurev-bioeng-071811-150124.
[60] S.A. Camacho, M.B. Kobal, A.M. Almeida, K.A. Toledo, O.N. Oliveira, P.H.B. Aoki, Molecular-level effects on cell membrane models to explain the phototoxicity of gold shell-isolated nanoparticles to cancer cells, Colloids Surf. B Biointerfaces 194 (2020), 111189, https://doi.org/10.1016/j.colsurfb.2020.111189.
[61] A.N. Bashkatov, E.A. Genina, V.I. Kochubey, V.V. Tuchin, Optical properties of human skin, subcutaneous and mucous tissues in the wavelength range from 400 to 2000 nm, J. Phys. D Appl. Phys. 38 (2005) 2543–2555, https://doi.org/10.1088/0022-3727/38/15/004.
[62] J.X. Xu, K. Siriwardana, Y. Zhou, S. Zou, D. Zhang, Quantification of gold nanoparticle ultraviolet-visible extinction, absorption, and scattering cross-section spectra and scattering depolarization spectra: the effects of nanoparticle geometry, solvent composition, ligand functionalization, and nanoparticle aggregation, Anal. Chem. 90 (2018) 785–793, https://doi.org/10.1021/acs.analchem.7b03227.
[63] A.G. Skirtach, A.A. Antipov, D.G. Shchukin, G.B. Sukhorukov, Remote activation of capsules containing Ag nanoparticles and IR dye by laser light, Langmuir 20 (2004) 6988–6992, https://doi.org/10.1021/la048873k.
[64] B. Radt, T.A. Smith, F. Caruso, Optically addressable nanostructured capsules, Adv. Mater. 16 (2004) 2184–2189, https://doi.org/10.1002/adma.200400920.
[65] R.R. Letfullin, C. Joenathan, T.F. George, V.P. Zharov, Laser-induced explosion of gold nanoparticles: potential role for nanophotothermolysis of cancer, Nanomedicine 1 (2006) 473–480, https://doi.org/10.2217/17435889.1.4.473.
[66] A.G. Skirtach, A. Muñoz Javier, O. Kreft, K. Köhler, A. Piera Alberola, H. Möhwald, W.J. Parak, G.B. Sukhorukov, Laser-induced release of encapsulated materials inside living cells, Angew. Chem. Int. Ed. 45 (2006) 4612–4617, https://doi.org/10.1002/anie.200504599.
[67] L. Galluzzi, I. Vitale, Molecular mechanisms of cell death: recommendations of the nomenclature committee on cell death 2018, Cell Death Differ. 25 (2018) 486–541, https://doi.org/10.1038/s41418-017-0012-4.
[68] B.V Parakhonskiy, W.J. Parak, D. Volodkin, A.G. Skirtach, Hybrids of polymeric capsules, lipids, and nanoparticles: thermodynamics and temperature rise at the nanoscale and emerging applications, Langmuir 35 (2019) 8574–8583, https://doi.org/10.1021/acs.langmuir.8b04331.
[69] A.G. Skirtach, P. Karageorgiev, M.F. Bédard, G.B. Sukhorukov, H. Möhwald, Reversibly permeable nanomembranes of polymeric microcapsules, J. Am. Chem. Soc. 130 (2008) 11572–11573, https://doi.org/10.1021/ja8027636.
[70] M.B. Oliveira, J. Hatami, J.F. Mano, Coatings cells using Layer-by-Layer deposition for cell encapsulation, Chem. Asian J. 11 (2016) 1753–1764, https://doi.org/10.1002/asia.201600145.
[71] R. Alzeibak, T.A. Mishchenko, N.Y. Shilyagina, I.V. Balalaeva, M.V. Vedunova, D. V. Krysko, Targeting immunogenic cancer cell death by photodynamic therapy: past, present and future, J. Immunother. Cancer 9 (2021), https://doi.org/10.1136/jitc-2020-001926.
[72] D.V. Krysko, A.D. Garg, A. Kaczmarek, O. Krysko, P. Agostinis, P. Vandenabeele, Immunogenic cell death and DAMPs in cancer therapy, Nat. Rev. Cancer 12 (2012) 860–875, https://doi.org/10.1038/nrc3380.
[73] S. Zhu, X. Wang, S. Li, L. Liu, L. Li, Near-Infrared-light-assisted *in situ* reduction of antimicrobial peptide-protected gold nanoclusters for stepwise killing of bacteria and cancer cells, ACS Appl. Mater. Interfaces 12 (2020) 11063–11071, https://doi.org/10.1021/acsami.0c00310.
[74] D.V. Volodkin, M. Delcea, H. Mohwald, A.G. Skirtach, Remote near-IR light activation of a hyaluronic acid/poly(L-lysine) multilayered film and film-entrapped microcapsules, ACS Appl. Mater. Interfaces 1 (2009) 1705–1710, https://doi.org/10.1021/am900269c.